Empirically derived connection design properties for *Guadua* bamboo

Trujillo, D & Malkowska, D

DOI 10.1016/j.conbuildmat.2017.12.065
ISSN 0950-0618
ESSN 1879-0526

Publisher: Elsevier

Empirically derived connection design properties for *Guadua* bamboo

Authors:

David J. A. Trujillo and Dominika Malkowska

Email and address

david.trujillo@coventry.ac.uk

Senior Lecturer
School of Energy, Construction and Environment
Faculty of Engineering, Energy and Computing
Sir John Laing Building
Coventry University
Priory Street
Coventry
CV1 5FB

Abstract:

Three connection design properties (dowel embedment strength, slip modulus and screw withdrawal capacity) were determined for one species of bamboo (*Guadua angustifolia* Kunth) using experimental methods adopted from timber engineering. 151 embedment strength and slip modulus tests were undertaken using smooth dowels with diameters ranging from 3 to 16 mm, whilst 240 screw withdrawal tests were undertaken using 3.5 to 5 mm diameter self-tapping screws. Using regression analysis, predictive equations for the three connection design properties were derived, based on fastener diameter, density and bamboo wall thickness. Coefficients of determination (R^2) ranged from 0.45 to 0.82. The predictive equations for embedment strength and screw withdrawal were adapted to output characteristic values and then compared to similar equations derived for timber contained in Eurocode 5, the latter would seem inappropriate for bamboo.

Keywords: Bamboo; timber; connections; embedment strength; slip modulus; screw withdrawal

Definitions and symbols

D	diameter of the culm
d	diameter of the dowel or outer thread diameter of screw
d_1	inner thread diameter of screw
F_{ax}	Maximum withdrawal load or withdrawal capacity of screw
f_{ax}	withdrawal parameter
f_h	Embedment strength
F_{yield}	Yield load
K_{ser}	Slip modulus
MC	moisture content
n	sample size
t	thickness of bamboo culm wall
ρ_k	characteristic density
ρ_m	mean density
ρ_{test}	density at the time of test
ρ_{12}	density adjusted to 12% moisture content

1. Introduction

Adoption of bamboo as a structural material has numerous environmental benefits, this is attributable to its fast growth and reproduction through rhizomes, resulting in a very effective carbon sink in well managed forests, with the potential to reduce pressure on other forest resources and substitute energy intensive products such as steel and concrete, and help recover degraded lands [1]. However, as stated by Janssen [2], making joints in bamboo is difficult due to its tapered, hollow, and not perfectly circular section, with nodes occurring at irregular intervals. Janssen adds that bamboo will only be truly accepted as a structural material once joint design has been resolved.

Since the beginning of the 21st century a number of test, design and construction codes or standards have emerged throughout the world, including an international design standard [3]. To the authors' knowledge only the Colombian design code (NSR-10) [4] contains any numerical values for joint design, and these are limited to *Guadua angustifolia* Kunth (*Guadua a.k.*) connected by through-bolts combined with mortar infilled internodes (Fig. 1). NSR-10 does not provide a process for derivation of these design values, and does not provide slip moduli, K_{ser}, either, without which accurate calculation of frame deformations is not possible. Research into bamboo joints, such as [5] has tended to focus on undertaking a small number of tests to determine the joint capacity for a configuration. This approach limits the reliable prediction and inference of joint capacities. More recent work has recorded other joint properties such as joint-slip and ductility, which are also required in design [6, 7], yet the size of the tested sample tends to be small ($n \leq 20$). Overall, an attempt to describe and quantify the mechanics of bamboo joints in a statistically rigorous manner is uncommon, and potential similarities to timber connection design theory are often overlooked. This paper seeks to address this shortcoming by attempting to edify a bamboo-specific approach for connection design using metal fasteners – specifically self-tapping screws, smooth dowels and bolts. Metal fasteners have been selected because of their ubiquity, ductility and potential to unleash innovation, though their applicability to bamboo should not be taken for granted – for example

common woodscrews and nails should be avoided as they can induce splitting in bamboo. In the context of this paper, connections are deemed to be a subset of joints. Connections are interpreted to be the specific location where two or more members are joined by means of a metal fastener.

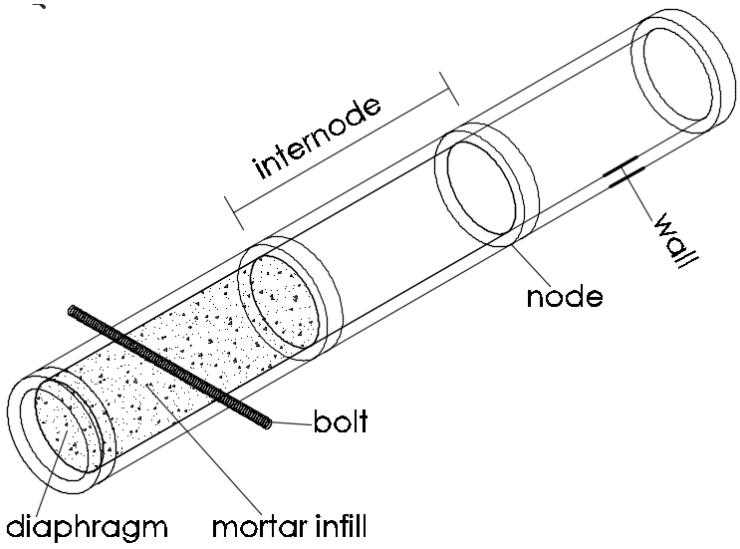

Figure 1: schematic representation of bamboo culm with through-bolt and mortar infill

1.1. Timber connection design theory

Design of connections using metal dowel-type fasteners in modern timber design codes e.g. Eurocode 5 (EC5) [8] are based on the European Yield Model (EYM). The EYM originates from Johansen [9] and is based on the plasticity of both the fastener and the timber in direct contact under the dowel, known as embedment, or dowel-bearing, strength, f_h. The model has been adopted because it provides a fairly accurate prediction of resistances and can be easily solved in a spreadsheet, however, it does not predict deformations or any other displacement related properties e.g. stiffness, ductility, or energy dissipation [10]. In terms of inference of joint stiffness – known as joint slip - Wilkinson [11] proposed one of the earliest models.

Use of the EYM is underpinned by a reliable knowledge of f_h. Eq. (1) was adopted in EC5 to infer f_h and was first proposed by Whale and Smith [12] following over 3200 tests to determine embedment properties and 420 full joint tests. The authors suggested that Eq. (1) was valid for softwood, hardwood and plywood. Empirical equations to infer the slip (or foundation) modulus, K_{ser}, have also

been derived. Eq. (2) from EC5 provides an estimate of K_{ser} for a range of dowel-type fasteners excluding driven nails.

$$f_{h,k} = 0{,}082(1 - 0{,}01d)\rho_k \quad N/mm^2 \quad (1)$$

Where: d is the diameter of the dowel type fastener, in mm; and ρ_k is the characteristic density for the timber strength class, in kg/m^3.

$$K_{ser} = \frac{{\rho_m}^{1,5} d}{23} \quad N/mm \quad (2)$$

Where: d is the diameter of the dowel type fastener, in mm; and ρ_m is the mean density for the timber strength class, in kg/m^3.

Another property useful to connection design is screw withdrawal capacity, F_{ax}. Blass *et al.* [13] derived Eq. (3) following 800 tests on spruce and screws with diameters ranging from 6 mm to 12 mm. This equation to infer the characteristic withdrawal capacity was adapted and incorporated into EC5. Blass and Frese [14] expanded the previous work to 1850 withdrawal tests with self-tapping screws with a range of diameters from 4 mm to 14 mm. Hubner [15] derived equations for screw withdrawal in hardwoods following 671 tests.

$$F_{ax,k} = \frac{0{,}52 \cdot \sqrt{d} \cdot {l_{ef}}^{0,9} \cdot {\rho_k}^{0,8}}{1{,}2 \cdot cos^2\alpha + sin^2\alpha} \quad (3)$$

Where: d is the diameter of the dowel type fastener, in mm; l_{ef} is the penetration length of the threaded part of the screw, in mm; ρ_k is the characteristic density for the timber strength class, in kg/m^3; and α is the angle between the screw axis and the grain direction.

Table 1 contains extant data for f_h in bamboo. Only Ramirez *et al.* [16] undertook regression analysis to determine equations that relate f_h to dowel diameter, however, unlike Eq. (1), the effect of density was not considered.

Table 1: Reported embedment strength values for bamboo

Bamboo species	Mean embedment strength parallel to fibres (N/mm^2)	Source:
Laminated *Guadua a.k.*	47.5 – 73.0	[16]
Gigantochloa atroviolacae	41.0	[17]
Bambusa pervariabilis	44.3	[18]
Guadua a.k.	43.5 – 74.7	[19], [20]

This paper contains proposed experimental methodologies for the determination of f_h, K_{ser} and F_{ax} for one species of bamboo and the empirical equations derived from the experimental results that could be employed in design, in a similar manner to Eqs. 1 – 3. The species used for all experimentation was *Guadua a.k.*, arguably the most important species from the structural perspective in Latin America.

2. Experimental Programme

2.1. General considerations

Currently there is no test procedure to determine connection design properties for bamboo, therefore a range of timber and bamboo standards were considered and adopted. The sample used was 4 m lengths of *Guadua a.k*. culms originating from the Colombian Coffee-region, the characteristics of the sample are listed in Table 2. The sample was stored in the Structures Lab of the Sir John Laing Building at Coventry University, an environment with a relatively stable temperature and relative humidity, this is evident from the range of moisture contents listed in Table 4. Unfortunately storage in a conditioning room at 20°C and 65% RH was not feasible. Specimens were extracted from the culms and then dimensioned using a band-saw.

Table 2: Test matrix

Sample size	*Embedment*			*Screw withdrawal*		
Distinct culm pieces	48			18		
Number of specimens	155			240		
Ages	*< 2 yrs*	*2-3 yrs*	*3-4 yrs*	*4-5 yrs*	*>5 yrs*	*unknown*
Embedment	50	27	23	15	31	9
Screw Withdrawal	36	54	41	40	69	0
Position along culm (from base)	*0 – 4 m*	*4 – 8 m*		*8 – 12 m*		*Unknown*
Embedment	48	55		43		9
Screw withdrawal	102	57		81		0

Density, ρ_{test}, was measured according to ISO 22157-1 [21] using the dimensions and mass at the time of testing. Moisture content, MC, was measured immediately before testing using an FMC Brookhuis moisture meter, the validity and calibration of this approach is discussed in [22]. Density values were adjusted to MC 12% by means of Eq. 4.

$$\rho_{12} = \rho_{test}\left[\frac{1.12}{1+w}\right] \qquad (4)$$

All testing was undertaken using a LLOYD LS100 designed for testing applications up to 100kN. For embedment tests data was recorded using a separate datalogger, load-cell and Linear Variable Displacement Transducers - LVDTs.

2.2. Embedment

The experimental work pioneered by Whale and Smith [23] used a full-hole procedure, similar to that contained in EN 383:2007 [24], to determine embedment properties. Whereas ASTM-D-5764 [25] makes an allowance for either a full-hole or a half-hole procedure. Franke and Magniére [26] discuss the merits of the half-hole and full-hole procedures and conclude the half-hole test provides a more realistic embedding strength, as it applies a more even stress, and hence suits the EYM better. However, they note, the full-hole test provides a more realistic stiffness for connections, as it includes the bending of the fasteners. Correal and Echeverry [19] adopted [25] for round bamboo

culms, using a dowel across a complete culm section as per Figure 2b. The two methodologies for dowel embedment were considered in this project. The full-hole methodology in accordance to [24] and the half-hole in accordance to [25]. As specimens were extracted from bamboo culms, not sawn timber, the configurations shown in Figure 2 were adopted.

An adaptation of [24] (Fig. 2a) was trialled, but significant fastener bending was evidenced. In the interest of determining more reliable embedment strengths, f_h, an adaptation of [25], similar to that used by Correal and Echeverry [19] was adopted. For dowels with a diameter, d, greater or equal to 6 mm a whole culm section with two half-holes was tested; procedure referred to henceforth as large diameter dowel (LDD) tests (Fig. 2b). For dowels with $d < 6$ mm, LDD tests proved problematic, therefore a culm segment with a single half-hole was tested instead. This procedure will be referred to as small diameter dowel (SDD) tests (Fig. 2c). Specimens were dimensioned as shown in Fig. 2, where: t is the wall thickness, d is the fastener diameter and D the diameter of the bamboo culm. Trujillo [20] had identified that placing a dowel at a node increased the embedment strength by about 30%, therefore specimens did not contain nodes in the proximity to the dowels in order to obtain a result that reflected a more likely scenario in design. SDD tests used common smooth nails. For LDD tests smooth steel dowels were fabricated. No dowel bending was observed in either half-hole procedure. Fig. 3 illustrates the specifics of the test set-up. Note that LVDT 1 was used to record dowel embedment, LVDT 2 was used to monitor any elastic shortening or settlement at the base, though this proved to be unnecessary. Table 3 summarises the characteristics of the sample tested.

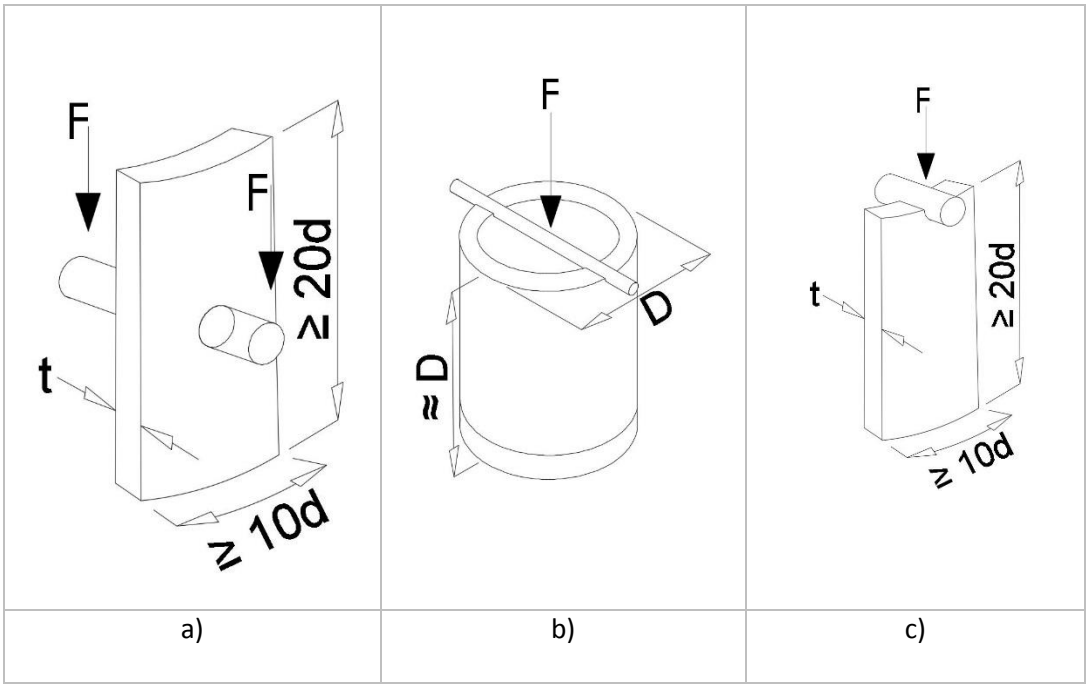

a) b) c)

Figure 2: Specimen (showing dimensions) adapted from: a) EN 383:2007, b) ASTM D 5764-97a for LDD and c) for SDD.

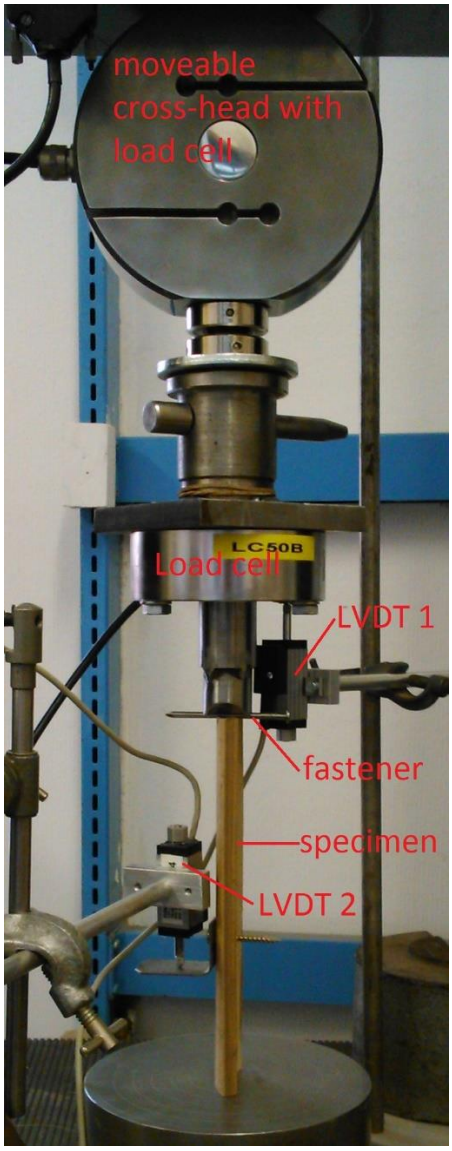

Figure 3: Set-up details, showing an SDD specimen

Table 3: test matrix for embedment tests

			n	Mean	CoV	Min	Max
Culm diameters, D		(mm)	155	101.2	14.1%	67.4	126.4
Wall thicknesses, t		(mm)		9.7	26.8%	6	15.8
Moisture content, MC		(%)		10.0	18.5%	7	15
Density at time of test, ρ_{test}		(kg/m^3)		770	11.4%	574	1060

d (mm)	**3 mm**	**3.45 mm**	**4.5 mm**	**6 mm**	**8 mm**	**12 mm**	**16 mm**
N	28	30	28	4	4	58	3

The nail or dowel was placed in the half-hole on top of the specimen and subjected to a compression force. The LVDT placed adjacent to the load-cell was used for recording dowel or joint slip. The test was performed at a constant rate of loading of 0.3 mm/min in order to meet the rate of loading requirements of [25]. Tests were terminated after 0.5d displacement. The slip modulus, K_{ser}, was interpreted as the slope of the linear part of the load-deformation curve, whilst the yield load, F_{yield}, was interpreted as per [25], which states that the yield point is interpreted as the point of interception between the load-deformation curve and a straight line offset by 5% of the dowel diameter from the linear part of the curve. . Embedment strength, f_h, was calculated from Eq. (5).

$$f_h = \frac{F_{yield}}{d \cdot t} \qquad (5)$$

2.3. Screw withdrawal

The methodology for screw withdrawal testing was based on EN 1382:2016 [27]. The bamboo specimen sizes matched those for SDD in Fig. 2. As the largest diameter screw considered was 5mm, a length of 100mm and outer arc of 50 mm was selected. After recording all measurements, the screw was driven perpendicularly to the specimen's convex surface, approximately at its centroid, ensuring the tip extended beyond the specimen, but the shank did not penetrate (Fig. 6a). The withdrawal force was applied along the fastener's axis and restraints were placed at $\geq 3d$ from the fastener's axis (Fig. 4b). Tests were performed with a constant rate of loading of 2 mm/min in order to reach the maximum force, F_{ax}, within 60 ± 15 s. The test was stopped when the load dropped to 80% of its maximum value. The withdrawal parameter, f_{ax}, was calculated from Eq. (6).

$$f_{ax} = \frac{F_{ax}}{d \cdot t} \qquad (6)$$

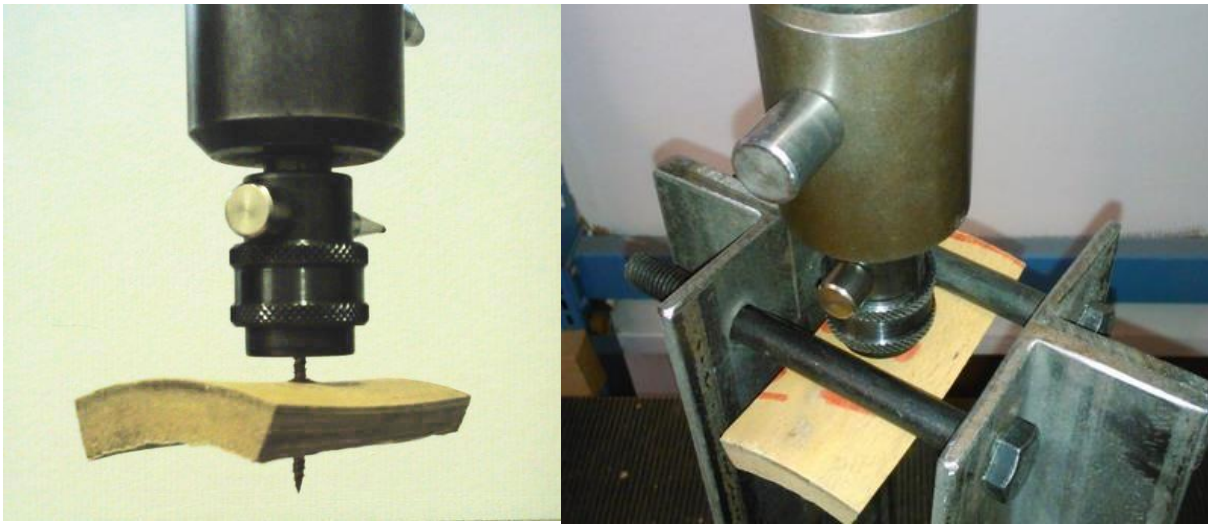

a) b)

Figure 4: set-up for withdrawal test a) close-up, b) showing restraints.

2.4. Screw types

Conventional woodscrews are likely to induce splitting in bamboo unless they are driven into pre-drilled holes, therefore the experiment focused on self-tapping screws, due to their simple installation. Three brands of self-tapping screws were tested. Prior to testing, the selected brands were vetted to ensure they did not induce splitting when fixed at 15 mm from the end (i.e. about 3*d* to 5*d*), which is less than EC5 requirements. The properties of the selected screws are summarised in Table 4 and the characteristics of the sample are summarised in Table 5.

Table 4: Properties of tested screws.

Screw ref.	Brand	Description	d (mm)	d_1 (mm)	pitch (mm)
3.5–b1	Brand 1: Turbo Gold®	Cutting edge tip, self-tapping woodscrew.	3.5	2.6	1.8
4.0–b1			4.0	2.7	1.9
5.0–b1			5.0	3.5	2.2
4.0–b2	Brand 2: Spax®	Serrated tip, self-tapping woodscrew.	4.0	2.5	2.3
4.8–b3	Brand 3: Easidrive®	Self-drilling roofing screw, with flanges filed down.	4.8	3.8	1.6

Table 5: characteristics of screw withdrawal test sample.

		n	Mean	CoV	Min	Max
Range of culm diameters, D	(mm)	240	105.3	14.8%	73.3	128.0
Wall thicknesses, t	(mm)		10.5	24.5%	6.0	15.0
Moisture content, MC	(%)		8.6	8.6%	7.2	10.3
Density at time of test, ρ_{test}	(kg/m^3)		755	11.2%	566	931

Screw ref.	**3.5–b1**	**4.0–b1**	**4.0–b2**	**4.8–b3**	**5.0–b1**
N	60	60	30	30	60

3. Embedment results

All bamboo specimens manifested primarily a bearing failure, though splitting during yielding was observed in two instances (Fig. 5). Fig. 6 displays the load-displacement curves for six specimens obtained from the same culm piece (culm piece reference: M12). These curves represent a range of post-yield behaviour, which could be characterised as oscillating around plasticity.

Table 6 summarises the experimental values from the embedment tests. Note f_h values are within the range of values listed in Table 1, and CoVs are within the range stated in [25]. Noticeably f_h seems to decrease with diameter, d (refer also to Fig. 7), which is in line with Eq. (1). Outliers were checked in IBM SPSS ® and identified with a circle. The software labels values more than 1.5× IQR (interquartile range) from the end of the box as outliers. On this basis some values were identified as outliers in Fig. 7 for f_h. However, other sources suggest 2.2× is a more valid approach for the determination of outliers [28]. On that basis there were no outliers present

Fig. 8 indicates that f_h does not seem to be strongly influenced by density, ρ_{12} . Fig. 9 indicates that slip modulus, K_{ser}, increases with d, which is in line with Eq. (2).

a) b)

Figure 5: a) Typical bearing failure, b) bearing failure with evidence of cracking.

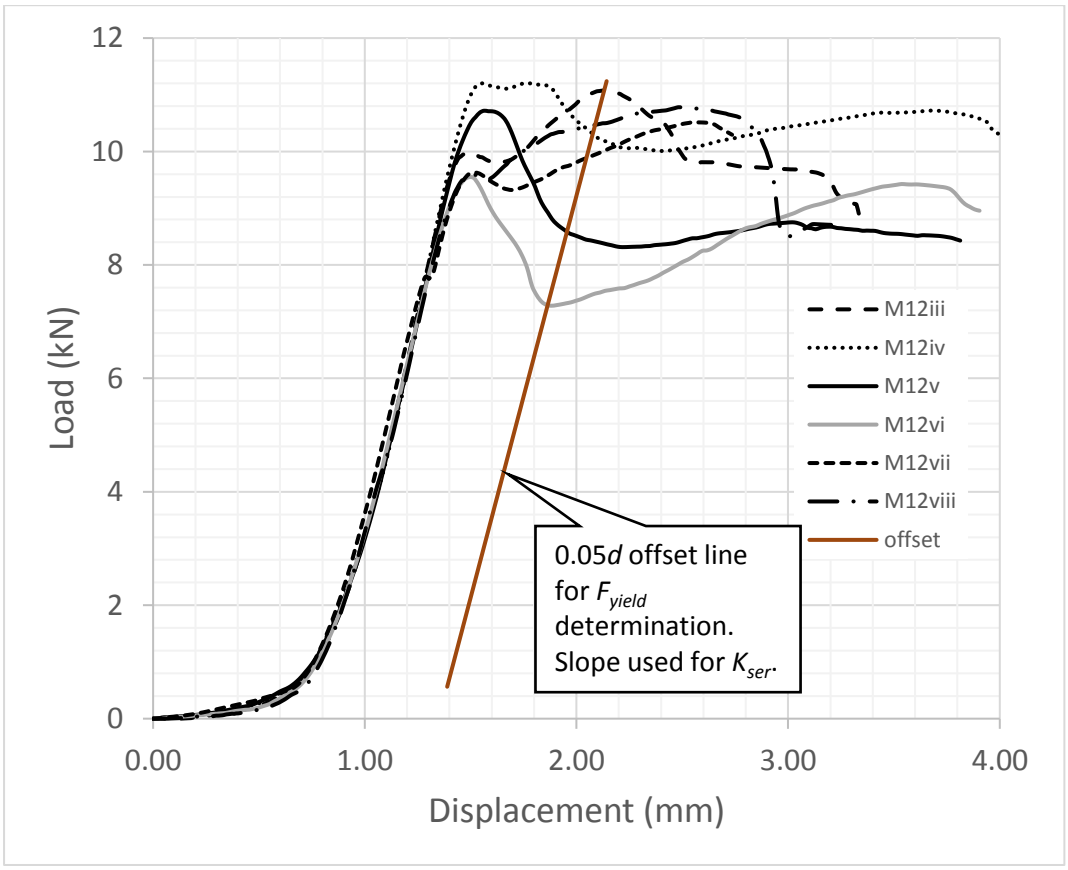

Figure 6: load-displacement graph for six specimens from the same culm

Table 6: summary of experimental results for embedment tests

d	n*	f_h		K_{ser}	
		Mean	CoV	Mean	CoV
(mm)		(N/mm²)	(%)	(N/mm)	(%)
3	28	62.4	24.0	5199	38.2
3.45	30	57.4	14.5	5810	37.4
4.5	28	58.2	17.1	6766	34.3
6	4	57.9	13.8	6388	17.5
8	4	53.3	15.4	9162	17.4
12	55*	48.7	18.9	12759	30.2
16	2*	37.1	12.1	12496	46.8
All	151	54.9	21.3	8589	51.0

* Sample size was revised to exclude data that was incomplete.

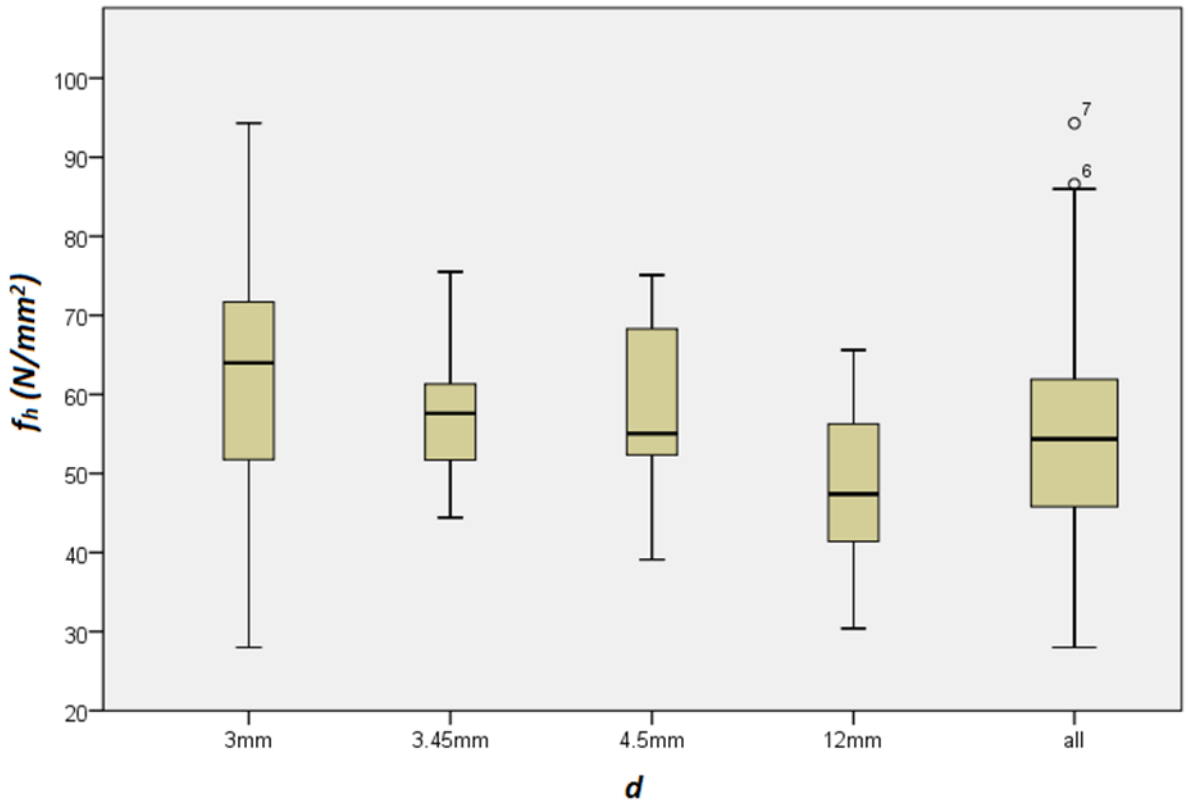

Figure 7: box-plot for f_h v d

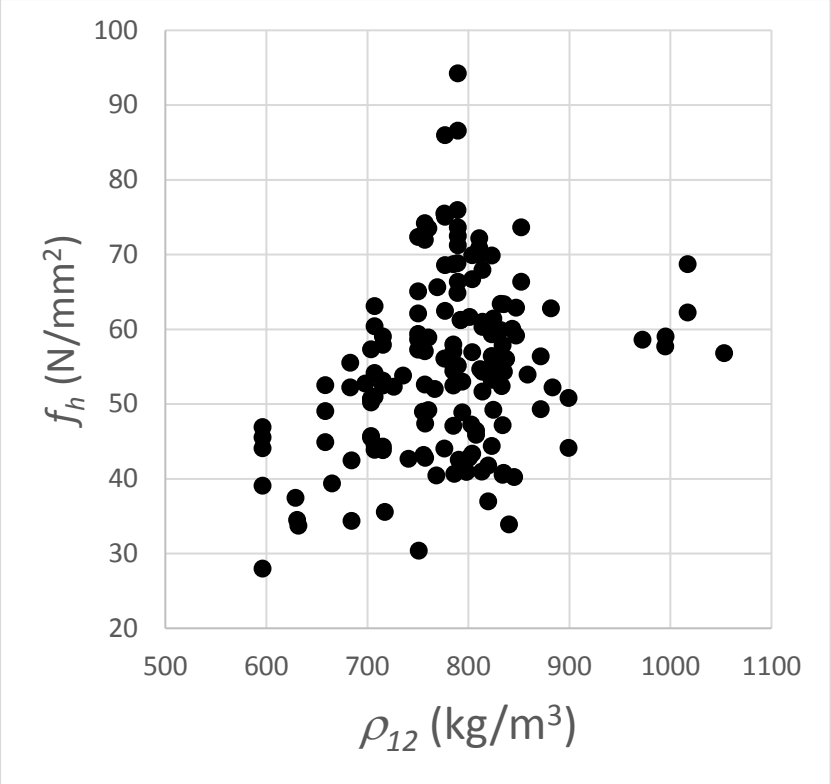

Figure 8: scatter graph for f_h

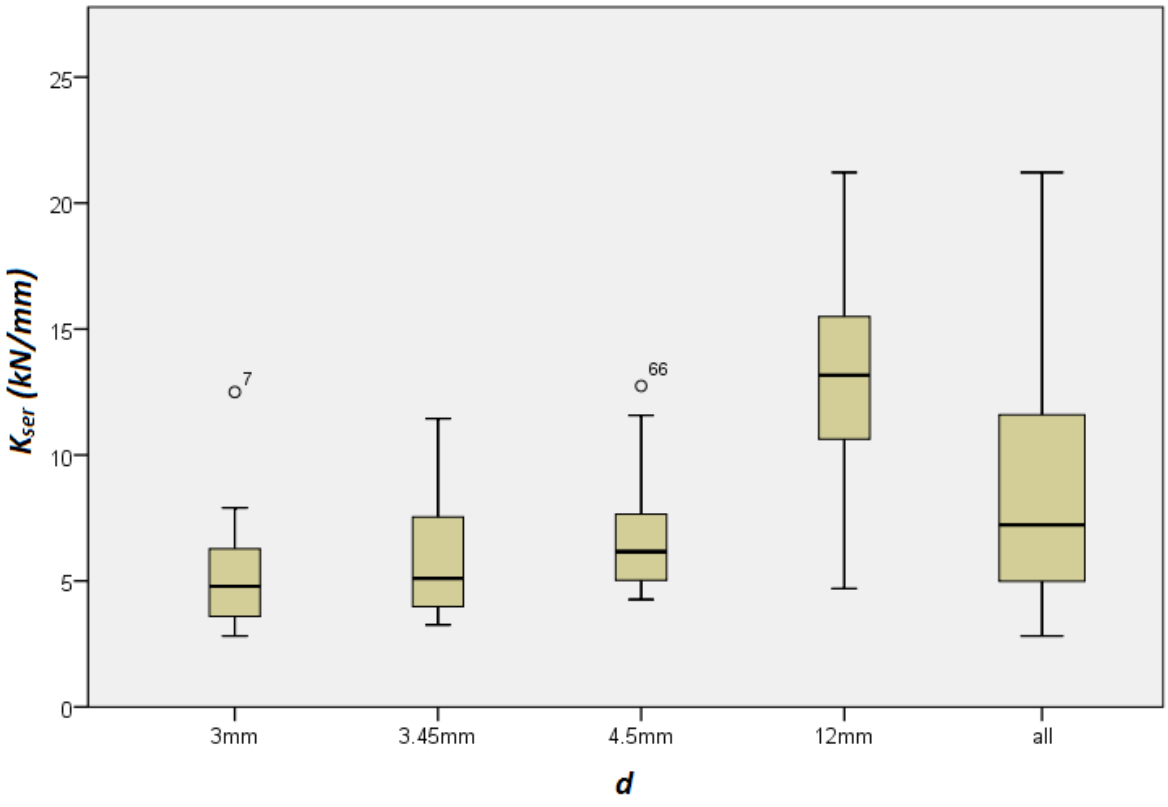

Figure 9: box-plot for K_{ser} per dowel diameter

4. Screw test results

The observed failure mode in all instances was pull-out of the screws (Fig. 10) in a fairly brittle manner (Fig. 11). Table 7 summarises the experimental values from the screw withdrawal tests. Evidently, withdrawal capacity, F_{ax}, increases with d. However, withdrawal parameter, f_{ax}, indicates that smaller diameter woodscrews perform the best (Fig. 12). Fig. 13 indicates that withdrawal parameter, f_{ax}, increases with ρ_{12}). Despite the indication in Fig. 12 that some values are outliers, they have not been excluded for the reasons presented in section 3. of this paper.

Figure 10: typical withdrawal failure mode

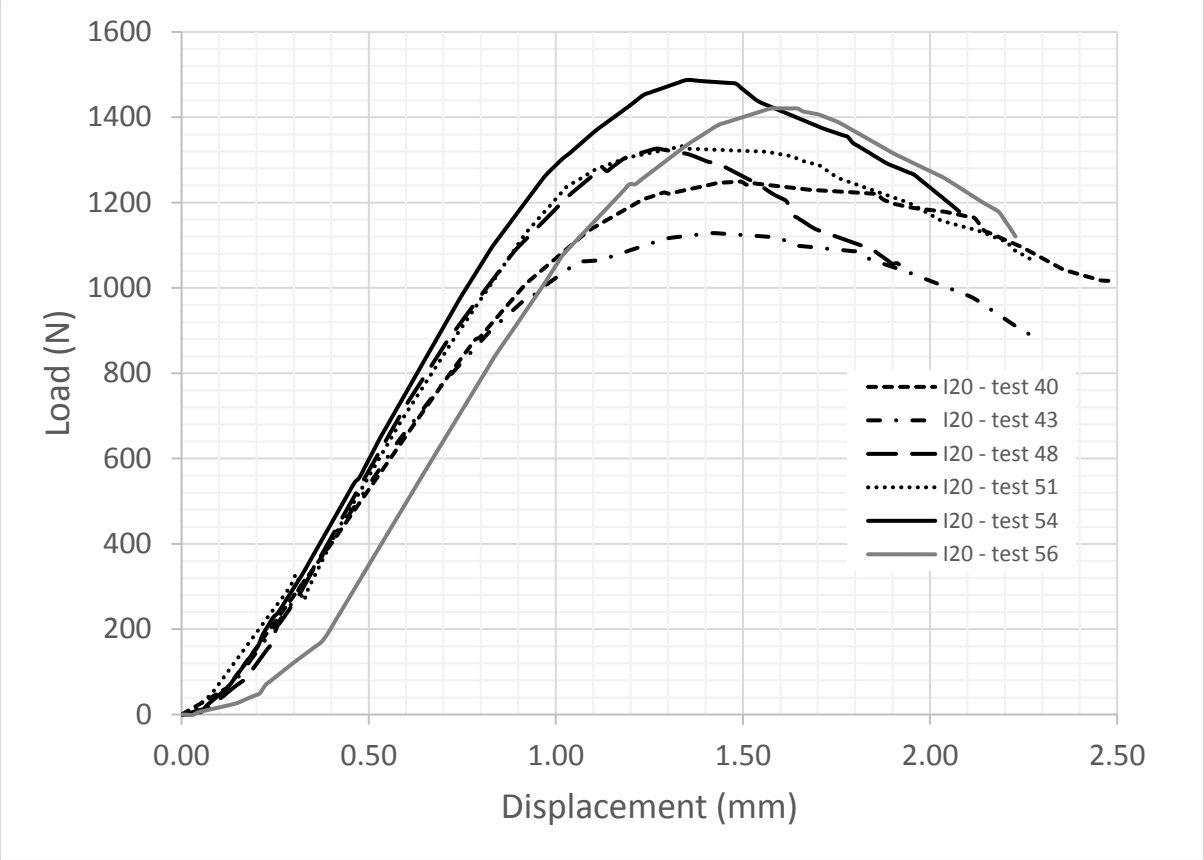

Figure 11: typical load-displacement graphs, these are for six specimens from the same culm

Table 7: summary of screw withdrawal tests.

Screw ref.	F_{ax}	CoV	f_{ax}	CoV
	(N)	%	(N/mm^2)	%
3.5–b1	1264	28.19	34.43	17.11
4.0–b2	1296	27.06	30.87	14.95
4.0–b1	1342	29.29	31.81	10.72
4.8–b3	1284	24.08	25.97	17.06
5.0–b1	1505	29.26	28.65	12.02
All	1350	28.94	30.83	16.85

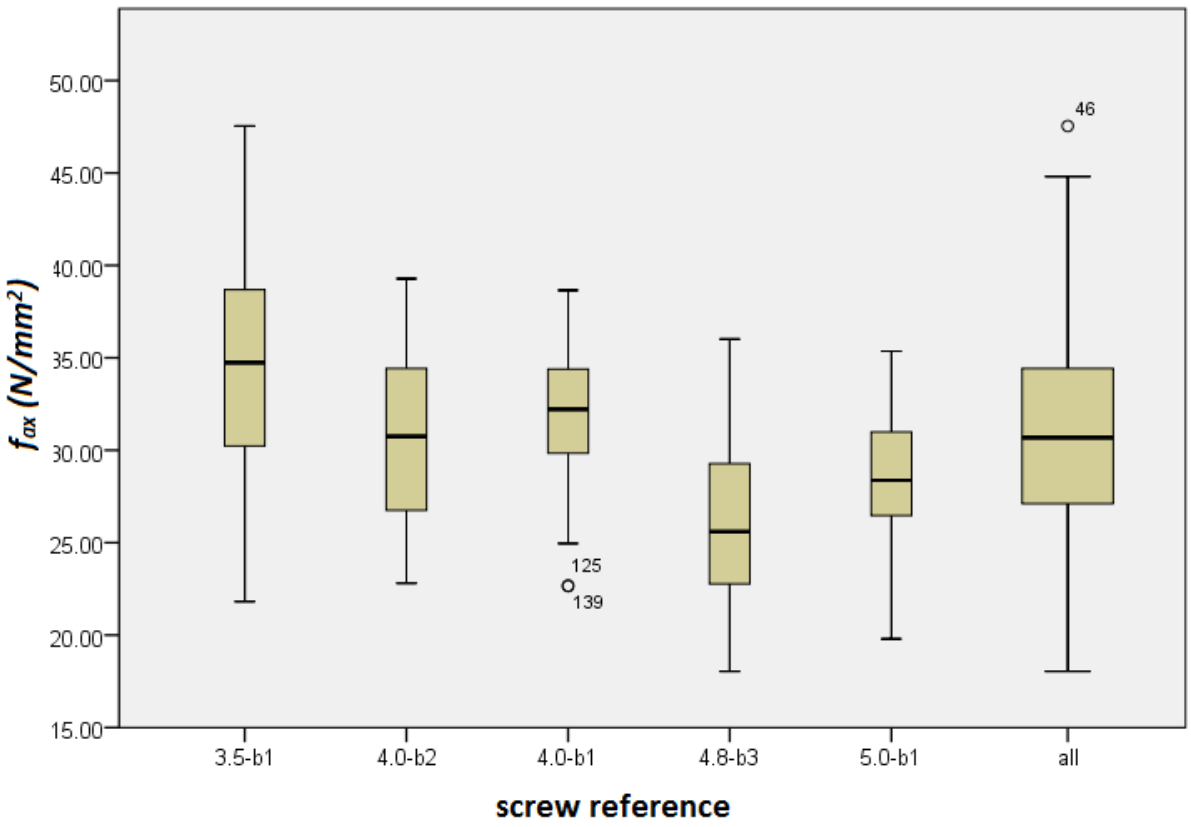

Figure 12: Box-plot for f_{ax} per screw type

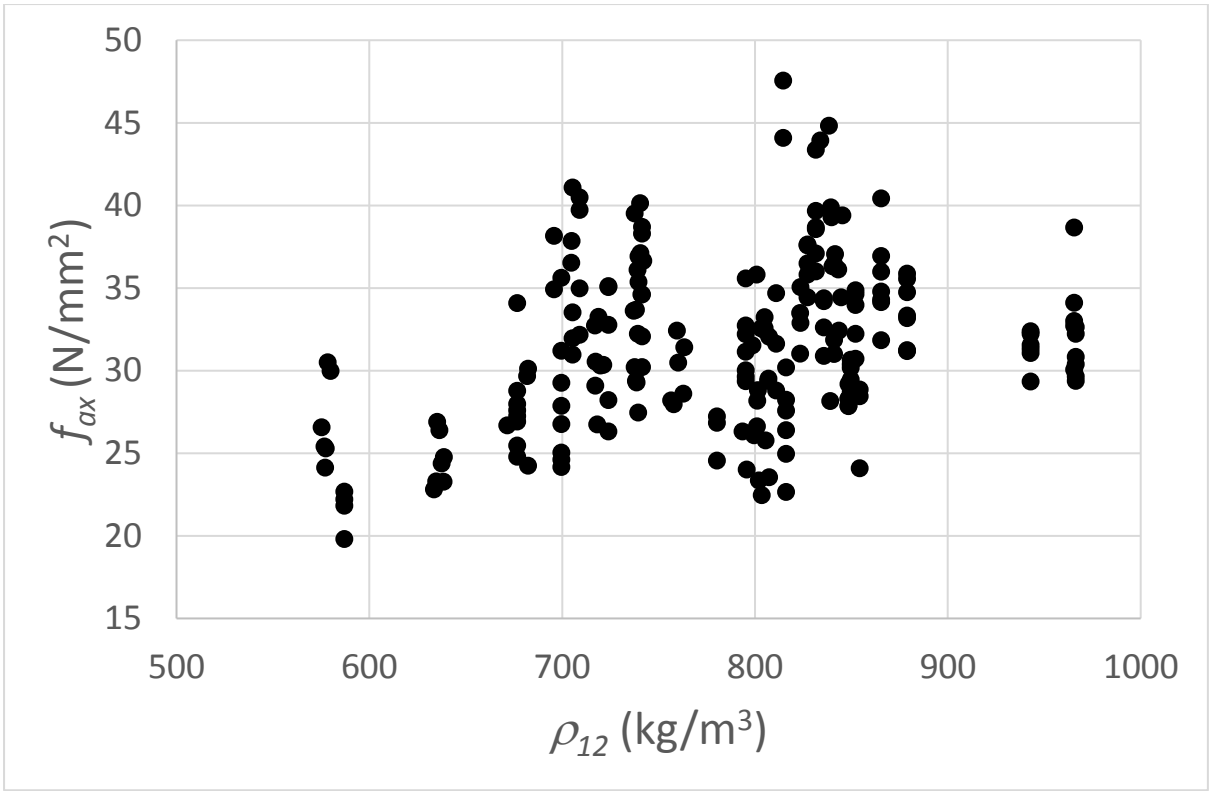

Figure 13: scatter-plot for f_{ax}

5. Effect of age and position

Bibliography compiled in Trujillo and Lopez (2016) [29] indicates that density and some mechanical properties increase along the culm, and that some mechanical properties are affected by the level of maturity at harvesting of the culm. Figs. 14 – 17 indicate the effect position along the culm and age at time of harvesting have upon f_h and f_{ax}. Figures 14 and 16 indicate that age and position the culm has no discernible or significant effect on f_{ax}. Figure 15 suggests that f_h peaks at around 2 – 3 years of age for *Guadua a.k*. which is not far removed from the observation made for compression parallel to fibres (which can arguably be linked to embedment) made by Correal and Arbeláez (2010) [30], which was that peak maturity occurred at 3 – 4 years. Fig. 17 indicates that there is a small link between position along the culm and f_h. This is in line with the findings from [30] for compression parallel to the fibres.

From these observations it may be concluded that f_{ax} is seemingly unaffected by age or position along the culm, whereas f_h obeys patterns observed for other mechanical properties such as compression. However, the authors have excluded data about position or age in subsequent analysis, as this information is not always readily available to fellow researchers or the end user.

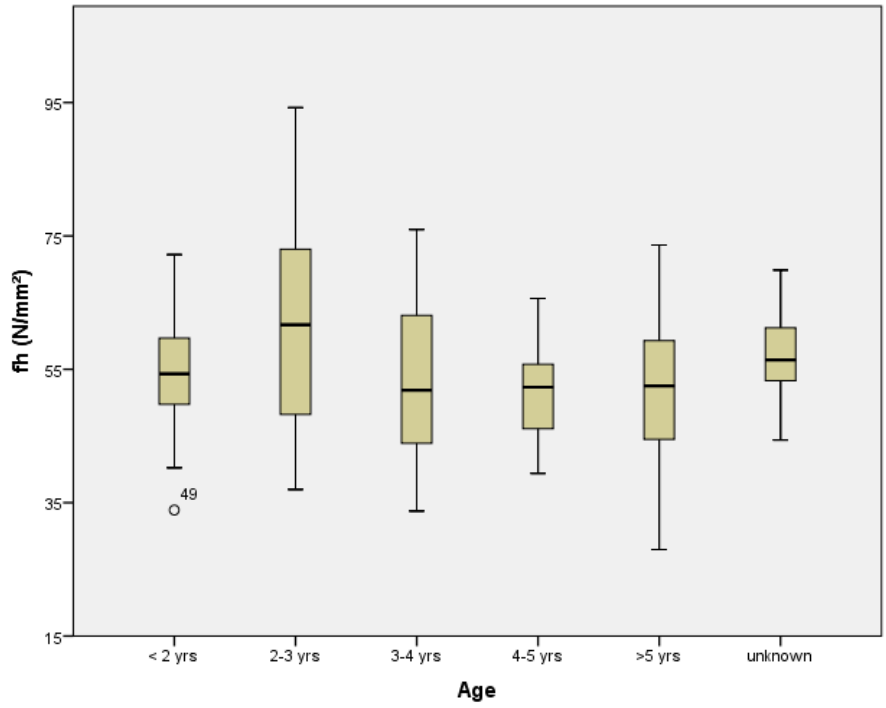

Figure 14: box-plot for f_h per age group

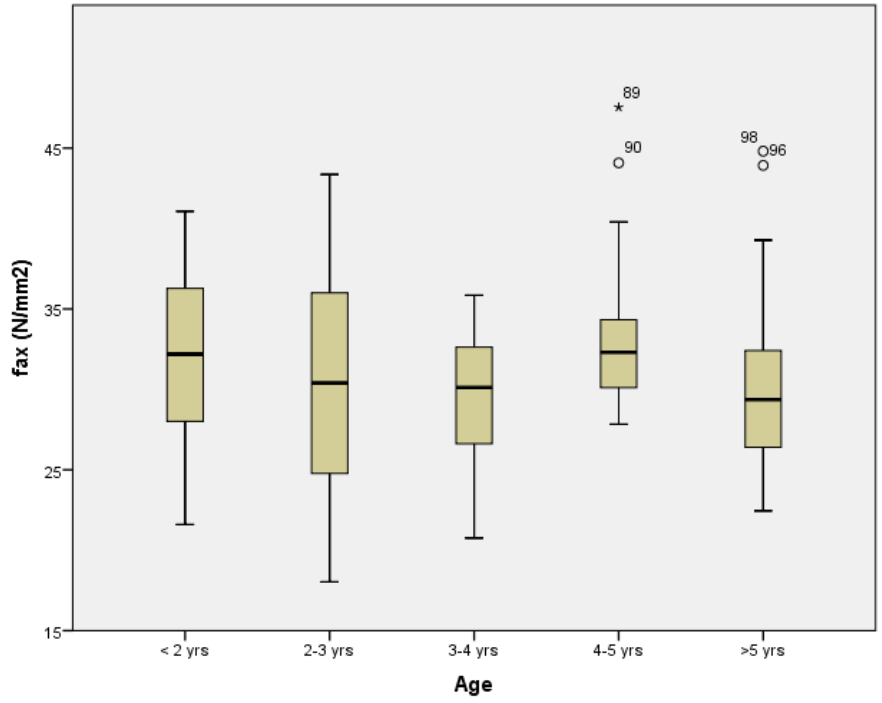

Figure 15: box-plot for f_{ax} per age group

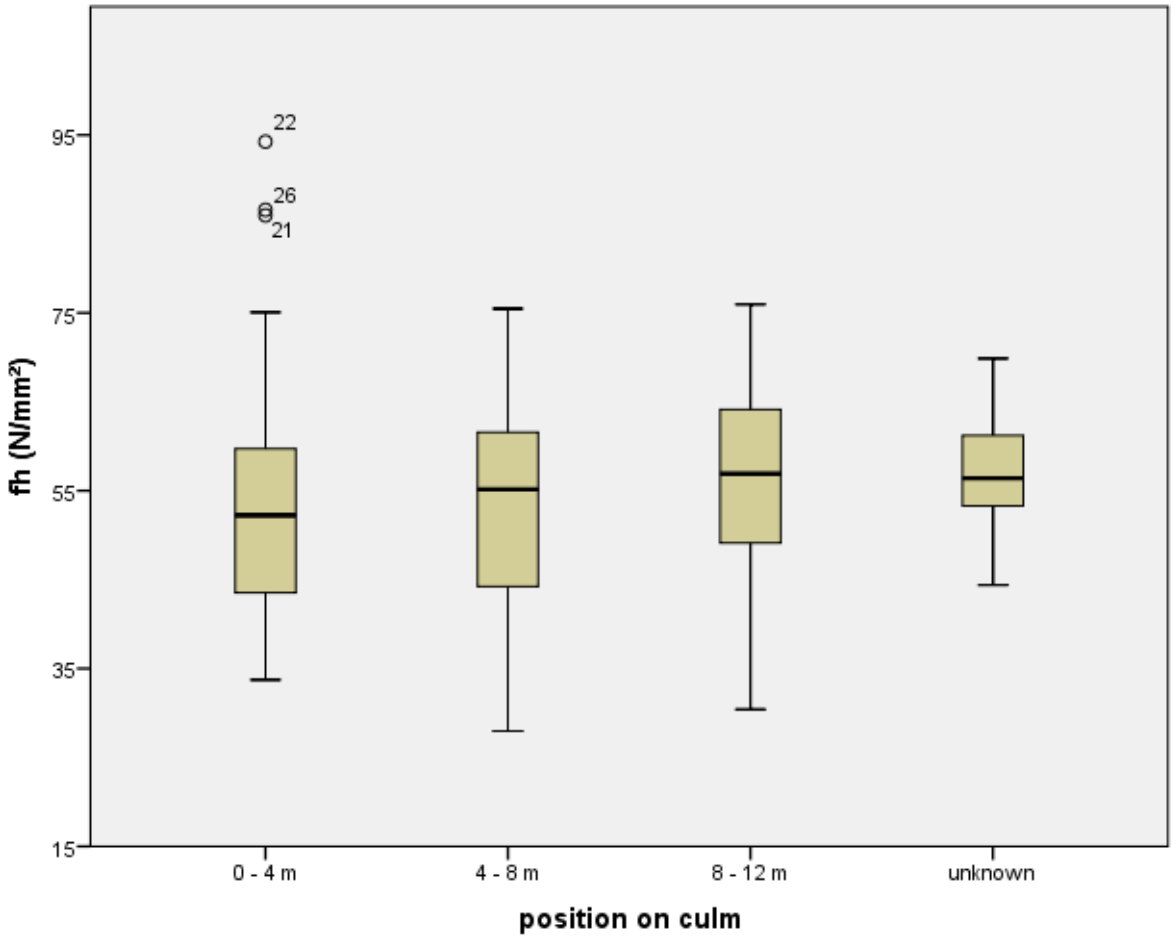

Figure 16: box-plot for f_h per culm position

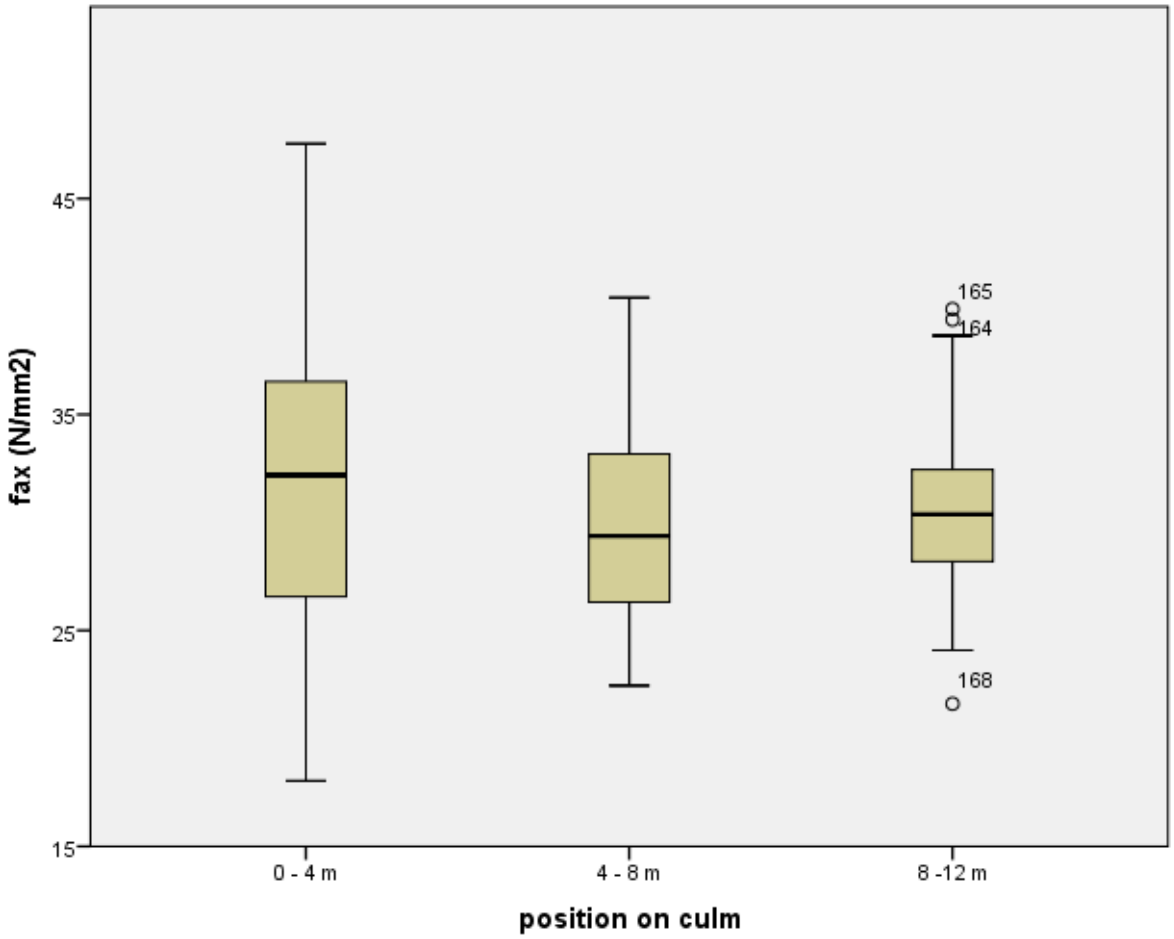

Figure 17: box-plot for f_{ax} per culm position

5. Discussion

5.1. Regression Analysis

One of the objectives of this project was to arrive at empirically derived equations for the inference of characteristic connection design properties ($f_{h,k}$, K_{ser}, $F_{ax,k}$, $f_{ax,k}$) for bamboo on the basis of easily determinable properties such as d, t, and ρ, in a similar manner as Eqs. (1), (2) and (3) are used in EC5. Multiple linear and non-linear regressions using Analysis of Variance (ANOVA) were run for each connection design property. The linear models investigated followed the form:

$$y = \beta_1 x_1 + \beta_2 x_2 + \cdots + \beta_{n-1} x_{n-1} + \beta_n x_{n_1}$$

Whereas the non-linear (power) models followed the form:

$$y = \alpha x_1^{\beta_1} \cdot x_2^{\beta_2} \cdot \ldots \cdot x_{n-1}^{\beta_{n-1}} \cdot x_n^{\beta_n}$$

In a similar manner to [13], the linear models explored, the aforementioned properties (*d*, *t* and ρ_{12}) were used as individual terms as well as their crossproducts and squares were included, as well as *MC*, arriving up to ten possible predictor variables altogether: *d*, *t*, ρ_{12}, $t \cdot d$, $t \cdot \rho_{12}$, $d \cdot \rho_{12}$, d^2, t^2, ρ^2, *MC*. In order to find the highest coefficient of determination (adjusted R^2) for a statistically valid model (*p*-values for all predictor variables ≤ 0.05), a script was written in Matlab® to compute R^2 for all possible combinations of the ten terms. Altogether, for 1023 combinations for the linear model were returned. For the non-linear models explored, the four individual terms (*d*, *t*, ρ_{12}, *MC)* were combined to produce up to 15 combinations. Table 8 summarises the empirical equations returned by the regressions with the highest adjusted R^2 and their respective adjusted R^2 values. In instances where the difference between the R^2 values for the linear and non-linear models was small, the latter were preferred on the basis of their simplicity. Note that R^2 values were much higher for F_{ax} ($R^2 \approx 0.83$) than for f_{ax} ($R^2 \approx 0.47$) for both linear and non-linear models, therefore only results for F_{ax} are listed. This is consistent with findings for timber [14]. Similarly, by excluding b3 screws (which are not wood screws) from the sample, R^2 values increased from ≈0.79 to ≈0.83. As specimens were not conditioned, their moisture contents were lower than 12% benchmark used in timber testing, therefore *MC* was included in the regression analysis to control for any influence that *MC* may have effected on connection design properties.

Figs. 18 a) b) and c) represent the observed (experimental) v predicted values for the three connection design properties. The model for F_{ax} provides the strongest correlation, whilst the model for f_h provides the weakest. The model for K_{ser}, may have been affected by the change in methodology from LDD to SDD tests. Similarly, the sample size for dowels between 4.5 mm and 12 mm was small, possibly creating a bias.

Table 8: equations for models returning highest R^2

Fastener property	Units	Equation	R^2	Equation Ref.
f_h	(N/mm^2)	$f_h = 0.058d^{-0.21} \cdot \rho_{12}^{1.09}$	0.4461	(7)
K_{ser}	(N/mm)	$K_{ser} = -1206.16 + 816.79MC - 1550.05d - 0.0127\rho_{12}^2 + 2.72\rho_{12} \cdot d + 0.7t \cdot \rho_{12}$	0.6935	(8)
F_{ax}	(N)	$F_{ax} = 0.03d^{0.53}\rho_{12}^{0.92}t^{1.19}MC^{0.48}$	0.8220	(9)
		Note: *d* and *t* in mm, ρ_{12} in kg/m^3, MC in %		

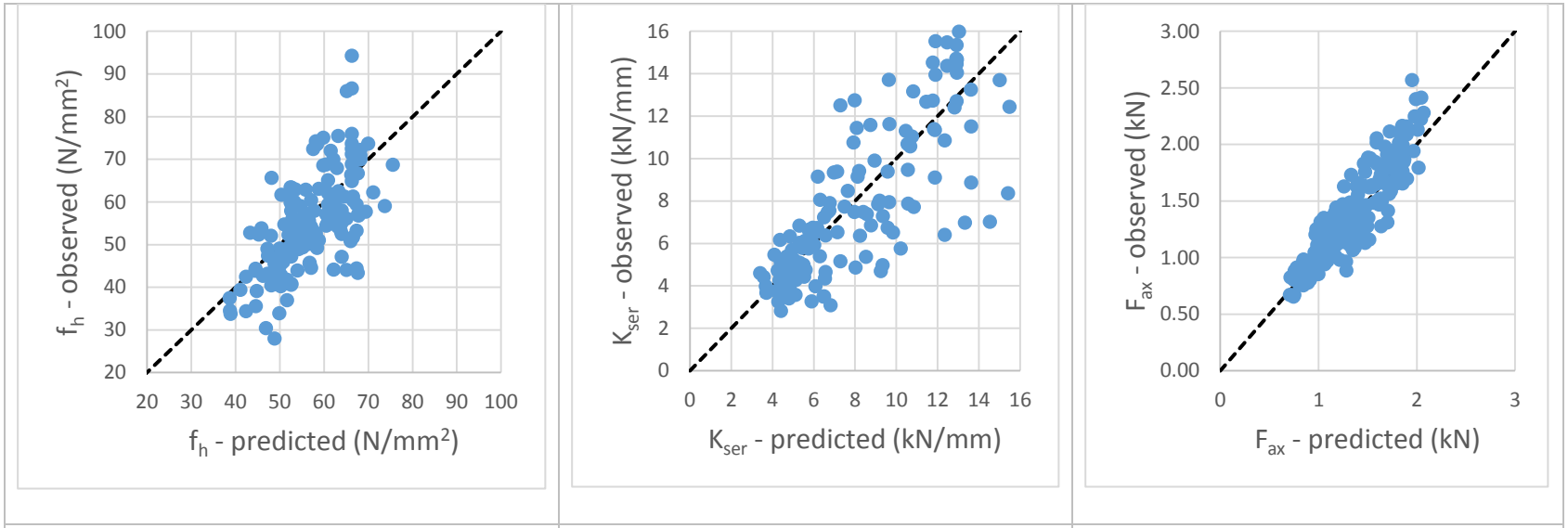

Figure 18: predicted v observed values for a) f_h b) K_{ser} c) F_{ax}

5.2 Characteristic values

The equations contained in Table 8 provide a prediction of the mean connection design properties. However, strength or capacity properties, such as f_h and F_{ax}, should be expressed as characteristic values for design purposes, as is the case for Eqs. (1) and (3). Connection design properties are calculated on the basis of characteristic density, ρ_k. According to EN 14358-2016 [31] characteristic values are determined at a confidence level equal to 75%. For simplicity, connection design properties and density were assumed to obey non-parametric distributions.

For density, Eq. (10) is used to obtain the 5-percent lower tolerance limit with 75% confidence, $\rho_{0.05}$ is the 5th percentile from ranked density data from each test; CoV and n, as defined in this paper; and $k_{0.05,0.75}$ is a multiplier to give the 5-percent lower tolerance limit with 75% confidence contained within [28]. The values for these are summarised in table 10.

$$\rho_k = \rho_{0.05}\left(1 - \frac{k_{0.05,0.75}CoV}{\sqrt{n}}\right) \quad (10)$$

By substituting ρ_k into Eqs. (7) and (9) the output values are now significantly reduced, however that does not necessarily warrant that their output would also be deemed a characteristic value. To assess this, the percentage of predictions that exceeded the experimental value, P_{fail}, was determined, and compared against a maximum permitted percentage of predictions that exceeded the experimental value, $P_{fail,pemit}$, which was found using the term contained within brackets of Eq. (10) and multiplying it by 5%. In this instance CoV was obtained from the ratio $f_{experimental}$ / $f_{predicted}$ for all values for the connection design property. If the check failed, the constant multiplier a from the non-linear equations (7) and (9) was modified until acceptance. Key steps and final equations are in table 9.

Table 9: final characteristic equations for connection design properties

Property	Units	$k_{0.05,0.75}$	ρ_k	$P_{fail,permit}$	Equation	*Eq ref.*	P_{fail}	$P_{fail,EC5}$
		-	(kg/m^3)	(%)	-		(%)	(%)
$f_{h,k}$	(N/mm^2)	1.84	621	4.88	$f_h = 0.051d^{-0.21}\rho_k^{1.09}$	(11)	3.97	26.49
K_{ser}	(N/mm)	-	ρ_{mean} = *780*	50	$K_{ser} = 6550 - 1550d - \rho_{mean}(0.013\rho_{mean} - 2.72d - 0.7t)$	(12)	49.67	15.23
$F_{ax,k}$	(N)	1.82	578	4.92	$F_{ax,k} = 0.083d^{0.53}\rho_k^{0.92}t^{1.19}$	(13)	4.81	66.35
	Note: *d* and *t* in mm, ρ in kg/m^3, MC in %							

It should be observed that Eq. (9) contains the term *MC* with a positive exponent. As this would indicate that at higher *MC*, higher F_{ax}, which is potentially misleading if extrapolated. Therefore, this term was substituted with the mean experimental *MC* for the Eq. (13).

5.3. Adoption of EC5

Adoption of Eqs. (1), (2) and (3) from EC5 in lieu of equations (11), (12) and (13) – contained in Table 9 - was investigated. $P_{fail,EC5}$ in table 9 indicates the percentage of predictions using the aforementioned EC5 equations that exceeded the experimental values. The outcome is that EC5 equations would output excessively high values for f_h and F_{ax}. Whereas in terms of K_{ser}, it would appear that EC5 underestimates stiffness. However, the equation for K_{ser} obtained in this paper is derived from a half-hole embedment test, which has limitations as discussed in 2.2.

5.4. Critique to yield criterion

It is noticeable from tables 6 and 7, that CoV for f_h (21.3%) is considerably higher than for f_{ax} (16.9%). As evidenced in table 2, numerous specimens were extracted from a single culm, particularly for screw withdrawal. In order to assess whether the higher CoV values for f_h were a consequence of the experimental method, or the larger variability within the sample selected, the authors analysed the

level of variation to either f_h (or f_{ax}) for specimens originating from a single culm piece. Wherever five or more specimens originated from the same culm segment and were tested with the same fastener, the coefficient of variation, CoV, for the respective connection design property (either f_h or f_{ax}) was assessed. Five groups of specimens for embedment and 11 for screw withdrawal were analysed and summarised in Table 10. On average, CoVs for f_{ax} ranged between 3.42% and 9.88%, whereas the CoVs for f_h ranged from 9.65% and 14.80%. This seems to imply that the embedment test, or possibly the interpretation of F_{yield}, results in more variable results. Fig. 6 suggests that the oscillations around the plastic behaviour compounded with the criteria used for the interpretation of F_{yield} could underlie this variability. To assess the effect the 0.05d offset criterion has on the data, the data for the five aforementioned groups of specimens for embedment were reanalysed using a range of offset criteria, ranging from 0% to 14%. It was found that an offset criterion of 0.12d resulted in an average CoV for f_h across the five groups of 8.31%, which is more in line with the CoV for f_{ax}. This possibility of adopting this offset criterion across all data was considered, but rejected on the basis of comparability with other published data.

Table 10: variation of connection properties within a culm

Test	CoV	f_h	f_{ax}
Embedment	Average	11.02%	
	Min	9.65%	
	Max	14.80%	
Screw withdrawal	Average		7.04%
	Min		3.42%
	Max		9.88%

6. Conclusions, recommendations and further work

As a contribution to the development of bamboo connection design theory, the basic properties for fastener-bamboo interaction were investigated for one species of bamboo (*Guadua a.k.*).

Experimental methods developed for timber were adapted for this purpose, with some success. However, the findings are yet to be validated with full-scale connection tests, such as two bamboo member joints and steel-bamboo joints. This is particularly important for the assessment of joint-slip. Interpretation of F_{yield} in embedment tests may underlie the higher levels of variability observed for embedment strength, f_h, when compared to the other properties assessed. Alternative definitions for f_h, such as those contained in [24] or ISO 10984-2:2009 [32], should be explored.

Seemingly, the age at the time of harvesting of the culms and position along the culm influenced f_h, but not withdrawal parameter, f_{ax}. Embedment of fasteners parallel to fibres exhibited some ductility, though splitting was observed in some instances. Screws subjected to withdrawal displayed little or no ductility.

Predictive empirical equations for bamboo connection design properties based on basic properties, such as ρ, d and t, were derived using regression analysis. R^2 values of 0.45, 0.69 and 0.82 were returned for f_h, K_{ser} and F_{ax}, respectively. These predictive equations were adapted to provide characteristic values, as per timber design codes. The obtained characteristic value equations differed significantly from those contained in Eurocode 5 for timber, which suggests that further work is required in order to derive bamboo specific connection design equations, similar to Eqs. 11, 12 and 13 in this paper, but based on a larger sample, an improved definition of f_h, subjected to more rigorous conditioning, and that includes a range of species

Further work regarding the compatibility of bamboo with metal fasteners is also recommended, in particular to assuage concerns about the risk of splitting when specimens are subjected to changes in temperature and moisture content.

Acknowledgement

The authors would like to thank Mr. Aaron Stanway, for undertaking some of the experimental work reported.

References

(1) Kuehl, L., Yiping, K., 2012. Carbon Off-setting with Bamboo. INBAR Working Paper 71. International Network for Bamboo and Rattan INBAR, Beijing, P.R. China.

(2) Janssen, J.J., 2000. Designing and building with bamboo - Technical Report 20. International Network for Bamboo and Rattan, Beijing, China.

(3) ISO (International Organization for Standardization), 2004. ISO 22156:2004 bamboo – structural design. Geneva.

(4) AIS (Asociación Colombiana de Ingeniería Sísmica), 2010. NSR-10-Reglamento colombiano de construcción sismo resistente - Capítulo G.12: Estructuras de guadua. Bogotá. (in Spanish)

(5) Farbiarz, J., 2001. Estudio sobre el Comportamiento de Conexiones con Guadua' (Study about guadua connection behaviour), Boletín técnico, Asociación Colombiana de Ingeniería Sísmica, p. 56 (in Spanish).

(6) Sassu, M., Andreini, M., De Falco, A. and Giresini, L., 2012. Bamboo trusses with low cost and high ductility joints. Open Journal of Civil Engineering, 2(04), p.229.

(7) Awaludin, A. and Andriani, V., 2014. Bolted bamboo joints reinforced with fibers. Procedia Engineering, 95, pp.15-21.

(8) CEN (European Committee for Standardization), 2014. EN 1995-1-1:2004+A2 - Eurocode 5: Design of timber structures - Part 1-1: General - Common rules and rules for buildings, Brussels.

(9) Johansen, K. W., 1949. Theory of timber connections. International Association for Bridge and Structural Engineering, Vol. 9, pp 249-262.

(10) Heine, C.P., 2001. Simulated response of degrading hysteretic joints with slack behavior (Doctoral dissertation, Virginia Polytechnic Institute and State University).

(11) Wilkinson, T.L., 1972. Analysis of nailed joints with dissimilar members. Journal of the Structural Division, 98(9), pp.2005-2013.

(12)Whale, L.R.S. and Smith, I., 1986. The derivation of design values for nailed and bolted joints in Eurocode 5. Proceedings of 19th CIB W18 Meeting.

(13)Blaß, H.J., Bejtka, I. and Uibel, T., 2006. Tragfähigkeit von Verbindungen mit selbstbohrenden Holzschrauben mit Vollgewinde., Bd. 4. Karlsruher Berichte zum Ingenieurholzbau. Universitatsverlag Karlsruhe, Karlsruhe. (in German)

(14)Frese, M. and Blass H.J., 2009. Models for the Calculation of the Withdrawal Capacity of Self-Tapping Screws. Proceedings of the 42nd CIB W18 Meeting.

(15)Hübner, U., 2013. Withdrawal strength of self-tapping screws in hardwoods. In Proceedings of the 46th CIB W18 Meeting.

(16)Ramirez, F., Correal, J.F., Yamin, L.E., Atoche, J.C. and Piscal, C.M., 2012. Dowel-bearing strength behavior of glued laminated Guadua bamboo. Journal of Materials in Civil Engineering, 24(11), pp.1378-1387.

(17)Awaludin, A., 2012. Aplikasi EYM Model Pada Analisis Tahanan Lateral Sambungan Sistim Morisco-Mardjono: Sambungan Tiga Komponen Bambu Dengan Material Pengisi Rongga, Proceedings of Nasional Rekayasa dan Budidaya Bambu Symposium, Yogyakarta. p 6. [in Indonesian]

(18)Paraskeva, T.S., Grigoropoulos, G. and Dimitrakopoulos, E.G., 2017. Design and experimental verification of easily constructible bamboo footbridges for rural areas. Engineering Structures, 143, pp.540-548.

(19)Correal, J.F. and Echeverry, J. S., 2015. Dowel-Bearing Strength Behaviour of Guadua angustifolia Kunth Bamboo. Proceedings of 16th NOCMAT conference, Winnipeg.

(20)Trujillo, D.J.A., 2009. Axially Loaded Connections in Guadua Bamboo. Proceedings of 11th NOCMAT conference, Bath.

(21) ISO (International Organization for Standardization), 2004. ISO 22157–1:2004 bamboo – determination of physical and mechanical properties – part I: requirements. Geneva.

(22)Trujillo, D., Jangra, S. and Gibson, J.M., 2017. Flexural properties as a basis for bamboo strength grading. Proceedings of the Institution of Civil Engineers–Structures and Buildings, 170(4), pp.284-294.

(23)Whale, L.R.J. and Smith I., 1985. A method for measuring the embedding characteristics of wood and wood-based materials, RILEM 57-TSB, Beit Oren, Israel.

(24)CEN (European Committee for Standardization) EN 383:2007 Timber Structures - Test methods - Determination of embedment strength and foundation values for dowel type fasteners. Brussels.

(25)ASTM International (1997) ASTM D 5764-97a Standard Test Method for Evaluating Dowel-Bearing Strength of Wood and Wood-Based Products, West Conshohocken.

(26)Franke, S. and Magniére, N., 2014. Discussion of testing and evaluation methods for the embedment behaviour of connections. Proceedings of the 47th CIB W18 meeting.

(27)CEN (European Committee for Standardization), 2016. EN 1382:2016 Timber Structures – Test methods – Withdrawal capacity of timber fasteners. Brussels.

(28)Hoaglin, D. C., and Iglewicz, B. (1987), Fine tuning some resistant rules for outlier labeling, Journal of American Statistical Association, 82, 1147-1149.

(29)Trujillo, D. and López, L.F. (2016) Chapter 13: Bamboo material characterisation in Nonconventional and Vernacular Construction Materials: Characterisation, Properties and Applications (editors: Harries, K.A. and Sharma, B.) Woodhead (Elsevier) Publishing. ISBN-13: 978-0-08-100038-0

(30)Correal J, and Arbeláez J (2010) Influence of age and height position of Colombian Guadua bamboo mechanical properties. Maderas: Ciencia y Tecnología, 12(2): 105-113, Chile.

(31)CEN (European Committee for Standardization) EN 14358-2016 Timber structures — Calculation and verification of characteristic values. Brussels.

(32)ISO (International Organization for Standardization), 2004. ISO 10984-2:2009 Timber structures — Dowel-type fasteners — Part 2: Determination of embedding strength. Geneva.